Archives Italiennes de Biologie, 148: XX-XX, 2010.

Virtual Brain Transplantation (VBT): a method for accurate image registration and parcellation in large cortical stroke

A. SOLODKIN[1], U. HASSON[2], R. SIUGZDAITE[1], M. SCHIEL[1], E.E. CHEN[1], R. KOTTER[3], S.L. SMALL[1]

[1] The University of Chicago, USA; [2] University of Trento, Italy; [3] Radboud University Medical Center Nijmegen, Netherlands

ABSTRACT

Objective: *The objective of the current study was to develop a semi-automated method to register and parcellate lesioned brains in a surface space with anatomical accuracy, facilitating group-level fMRI analyses in patients with large cortical strokes.*

Methods: *Thirteen chronic patients with a single large left hemisphere stroke were included in the study. Our "virtual brain transplantation" (VBT) approach is based on pre-processing high resolution anatomical T1-weighted brain images by "filling in" the lesion with "transplanted virtual tissue" from the non-stroke hemisphere, providing "normal" anatomical landmarks for standard alignment and inflation algorithms developed for healthy individuals. Biological validation of the approach was performed by quantifying in Freesurfer space the areas of 12 hand-drawn sulci found inside and outside the stroke following "transplantation".*

Results: *Our results show no difference in the Freesurfer parcellation of 12 different regions when comparing a lesioned hemisphere with the non-lesioned hemisphere, attesting for the validity of the anatomical classification in the stroke hemisphere. As consequence of the anatomical precision, this method permits a more detailed and quantifiable anatomical description of the regions affected directly by the stroke.*

Conclusions: *This method permits accurate surface reconstruction of the injured hemisphere after stroke by making it possible to extract the cortical surface from these images and to utilize this in software modules (FreeSurfer) specialized for aligning cortical surfaces using high-dimensionality warping algorithms. In addition, it permits quantifying, within bounds, the extent to which the lesion in question is associated with damage to particular regions of the cortical surface, information that is of explanatory value in models that attempt to explain brain-behavior relations using lesion analysis.*

Key words

Mancano

Introduction

The work of Ramon y Cajal represents a remarkable example of the importance of anatomy to the understanding of function in the central nervous system. The neuron theory that gained him the Nobel Prize in Medicine or Physiology was based exclusively on anatomical observations (Ramon y Cajal, 1899-1904), and since that time, anatomy and physiology have been inextricably linked in the study of the nervous system. The past century has seen remarkable strides in methodological development for brain physiology. Due to the invasive nature of many of these novel techniques, studies related to

Corresponding Author: Ana Solodkin, PhD, Department of Neurology, MC 2030, The University of Chicago Hospitals, 5841 S Maryland Ave, Chicago, IL 60637 - Email: solodkin@uchicago.edu

brain function in humans were limited originally to the investigation of individuals with naturally occurring lesions (Aharonov et al., 2003), only later supplemented by functional techniques such as electroencephalography (EEG). Despite the usefulness of these approaches, their limitations are significant, since neither lesion analysis nor EEG provides sufficient anatomical or functional resolution to ascertain neural mechanisms.

The development of imaging techniques, particularly magnetic resonance imaging (MRI), has brought about for the first time the tremendous opportunity to study the organization of the human brain noninvasively and with high anatomical and functional resolution (Raichle, 1998; Beaulieu, 2002; Tovino, 2007; Gjedde, 2008).

Among the most common MRI methods currently used by the neuroscience community to study brain function is functional MRI (fMRI), a method based on levels of blood oxygenation (Marcar and Loenneker, 2004; Goense and Logothetis, 2008; Yesilyurt et al., 2010), related (albeit indirectly) to neuronal activation (Marcar and Loenneker, 2004; Goense and Logothetis, 2008; Yesilyurt et al., 2010). This has allowed researchers to characterize brain activation patterns related to different environmental inputs and behaviors (Hennig et al., 2003). Although early fMRI studies did not address to a significant degree the anatomical issues related to their functional investigations, the increase in resolution of structural MR images combined with the need for an accurate description of the location of observed activations led the field to consider more careful anatomical analyses (Roland and Zilles, 1994; Kotter and Sommer, 2000; Toga et al., 2006), and to link functional activations to anatomical landmarks when applicable. In the words of Toga and Thompson (2007) “knowledge of the anatomy may be tedious to learn but it is clearly needed and no less important than all the elements of the experiment and analysis, the imaging protocol, the mathematics, the reference(s) and the visualization”. The anatomical approach espoused by many included the proper classification of brain regions to be used as references for describing brain regions associated with specific patterns of activation.

In this context, classifying and labeling brain regions has been an integral part of fMRI research, and has helped to improve our understanding of brain physiology. Consequently, the development of explicit methods for parcellating gray and white matter has helped establish a common reference frame across studies from which it is possible to determine functional principles from fMRI observations, pathway tracing, to network modeling (Sporns et al., 2005; Biswal et al., 2010; Kennedy, 2010).

The focus on anatomical precision is laden with particular difficulties due to the tremendous anatomical variability among individuals in both size and topology, especially at the level of the cerebral cortex (Paus et al., 1996; Le Goualher et al., 1999; Chiavaras et al., 2001; Damasio, 2005). Perhaps the most prevalent method for assessing anatomical features in individual images has been to spatially normalize brains into some type of stereotactic anatomical common space. An early and extensively used example is the Tailarach and Tournoux atlas, which famously lacks resolution.

To increase anatomical precision, newer approaches based on either an automatic brain surface registration or on a semiautomatic landmark alignment have been implemented for MRI analysis. These software packages include Caret (Van Essen and Dierker, 2007); http://brainvis.wustl.edu, Brain Suite (Shattuck et al., 2009); http://www.loni.ucla.edu/Software/BrainSuite), BrainVoyager (Goebel et al., 2006); http://www.brainvoyager.com and Freesurfer (Dale et al., 1999; Fischl et al., 1999); http://surfer.nmr.mgh.harvard.edu/), all of which permit the registration, segmentation and subdivision of the brain, and in some cases, white matter.

Independent of the parcellation method used, these approaches all require the input of intact brain images with all structures present. Hence, their use has been limited essentially to healthy individuals. However, remarkable efforts have been made recently to apply normal group-population atlases to the registration and parcellation of the brains of individuals with diseases such as Alzheimer’s Disease and schizophrenia (Toga et al., 2001). Although in the case of Alzheimer’s Disease, brain anatomy can be atrophic and even deformed in extreme cases, it does not include absence of specific brain regions (Van Hoesen et al., 1995). A different situation arises when pathology includes space-occupying or destructive (structural) lesions, where parts of the brain are missing. The most prevalent examples of acute destruction lesions are cerebrovascular infarc-

tions (strokes). In the case of large strokes, the use of automatic parcellation has been difficult due to the large amount of missing tissue combined with the *ex vacuo* changes to the remaining ipsilateral tissue, which can be atrophic and distorted (Bucy, 1964; Warabi et al., 1990; Graham and Landtos, 2002; Kabir et al., 2007).

Consequently, the anatomical approach to the study of large populations of stroke cases with extensive cortical lesions has been problematic. Basically, there have been two different anatomical methods used in stroke: 1) The first uses direct registration to existing reference atlases. Such registration, e.g., to Talairach space using Cost-function masking lacks precision, as noted previously (Thompson et al., 1996; Dinov et al., 2000). 2) The second uses semi-automatic methods based on registration to hand-drawn sulci. This approach, albeit very precise, is extremely time consuming, making it difficult to study large groups and/or to perform group analysis (Fiez et al., 2000). A recent report (Nachev et al., 2008) based on an idea by Weiller (1995) describes a computational method to facilitate the use of registration methods in SPM by filling the lesion produced by the stroke with tissue from the contralateral hemisphere. While this method allows alignment of brains with extensive lesions, it relies on the assumption of symmetry between hemispheres, and was tested only in intact brains with artificially superimposed lesions on one of their hemispheres.

However, there is much less natural asymmetry between hemispheres in stroke patients than in healthy individuals (Watkins et al., 2001), not only because of non-uniform atrophy as direct consequence of the stroke (Bucy, 1964; Warabi et al., 1990; Graham and Landtos, 2002; Kabir et al., 2007) but also because of age-related changes in the stroke survivors who tend to be older (Arnold et al., 2008; Gonoi et al., 2009; Nagai and Kario, 2009). The present work sought to overcome this limitation in a novel method for stroke patients with large cortical strokes.

The objective of the current study was to develop a semi-automated method to register and parcellate lesioned brains in a surface space with anatomical accuracy, facilitating group-level fMRI analyses in patients with large cortical strokes. Our "virtual brain transplantation" (VBT) approach is based on pre-processing high resolution anatomical brain images by "filling in" the lesion with "transplanted virtual tissue" from the non-stroke hemisphere, providing "normal" anatomical landmarks for standard alignment and inflation algorithms developed for healthy individuals. This method permits accurate surface reconstruction of the lesioned hemisphere after stroke by making it possible to extract the cortical surface from these images and utilize this in software modules (FreeSurfer) specialized for aligning cortical surfaces using high-dimensionality warping algorithms. In addition, it allows for quantifying, within bounds, the extent to which the lesion in question was associated with damage to particular regions of the cortical surface, information that is a useful explanatory factor in models that attempt to explain lesion-behavior relations.

Methods

Pilot study

Large cortical lesions from adult stroke patients were used to create simulated lesions on high-resolution T1 volumetric scans of non-infarcted brains. A variety of lesions were hand drawn on the 3D volume representations of the brains of 14 healthy subjects (one lesion per brain), creating "simulated lesions". A "virtual brain transplant" was then performed on each brain using one of two sorts of virtual brain matter: (a) simulated white and gray matter extracted from the corresponding regions of a standard Talairach and Tournoux Template-TTatlas (AFNI) (Talairach and Tournoux, 1988), or (b) the analogous area from the opposite hemisphere of the individual brain. An exact hand-drawn mask of the lesion was used to extract the selected VBT tissue, followed by the creation of a dataset in the same space as the original, but with virtual brain tissue transplanted into the lesion space (Wier et al., 2006).

VBT computational validation

Internal comparison (simulated lesion, Talairach, and homologue *vs.* original)

To assess the accuracy of the TTatlas as compared with the homologue VBT and simulated lesion, we used FreeSurfer to inflate and parcellate (a) the original brain (without lesions), (b, c) the two brains with the simulated lesion and transplanted tissue (TTatlas and homologue), and (d) the brain with the

unfilled simulated lesion. Freesurfer was used to parcellate the original (unlesioned) brain 100 times to factor out differences due to normal variance in the program. Variance in the size of each region was then calculated for each of the 100 permutations. Finally, automated parcellation was applied to each of the brains with simulated lesions, and in each case, the size of the regions was plotted against the normal variance of the parcellation program on the original unaltered brain image. Median scores were much higher with the homologous (79%) than with the TTatlas (52%).

External comparison (VBT *vs.* cost-function masking in SPM)

To assess the amount of displacement introduced by the method and compare our method to an alternative method, we aligned the VBT brains using either the FreeSurfer pipeline or Cost-function masking (Crinion et al., 2007) as implemented by SPM99. On each brain we marked the premotor region (ROI) in each participant's original space and registered it to common space using either the original non-lesioned brain or the lesioned brain that was registered to common space using FreeSurfer or Cost-function Masking. We then evaluated the accuracy of registration by calculating the percent overlap between the marked ROI's location in common space (a gold standard established using the non-lesioned brain) and the location of the same ROI when transformed to common space using VBT or Cost-function masking. The data were normalized by the volume of false positives, using the following algorithm:

Accuracy index = (true hits) - (false positive hits)*

Where:

True hits = number of voxels shared by normal and VBT brain/number of voxels in VBT

False positive hits = number of voxels in normal brain/(total voxels - number of voxels in VBT brain)

* The same procedure was used to assess the VBT and the Cost-function approach.

The Wilcoxon signed rank test was conducted to test whether there was a difference between the VBT and the Cost-function masking accuracy index data.

Stroke study

Participants

Thirteen patients were recruited from various hospitals and rehabilitation facilities in the Chicago area for a study of post-stroke aphasia therapy. All patients were at least 6 months post-stroke, and the presence of a single left hemisphere stroke was documented by history and brain imaging (structural MRI taken at the beginning of the research study). The group consisted of 10 males and 3 females with a mean age of 52.8 years (range 31-71), and all were right handed as assessed by the Edinburgh handedness inventory (Oldfield, 1971). Anatomically, all participants had large lesions in the distribution of the left middle cerebral artery. The Institutional Review Board of The University

Table I. - Demographical and neurological data for the stroke participants in the study.

Patient	Age	Gender	Stroke volume (number of voxels)	Percent of hemisphere lesioned	Stroke location
001	71	F	44,341	9.6	Frontal-insular-parietal
002	65	M	46,748	9.7	Frontal-insular
004	63	M	52,718	7.5	Frontal-temporal-insular
005	55	M	23,034	3.3	Frontal-temporal-parietal
006	65	M	40,286	6.4	Frontal-temporal-parietal
009	44	F	110,725	17.9	Frontal-temporal-parietal-occipital
010	31	F	74,528	10.6	Frontal-insular-temporal-parietal
011	58	M	150,500	19.8	Frontal-insular-temporal-parietal
013	36	M	93,378	12.4	Frontal-insular-temporal-parietal
014	33	M	67,567	10.1	Temporal-insular-parietal-occipital
015	61	M	183,780	26.3	Frontal-insular-temporal-parietal
016	57	M	24,050	3.2	Frontal-insular-temporal
017	47	M	82,949	13.5	Frontal-insular-temporal-parietal

of Chicago approved the study, and all participants provided written informed consent. Demographics of our cohort are summarized in Table I.

Image acquisition and data analyses

Patients were scanned in a 3T Siemens Trio scanner (at Northwestern University, Chicago), with a standard head coil. A volumetric T1-weighted scan (matrix 256 x 256 mm, 176 slices, 1 x 1 x 1 mm, 1 mm gap, TE = 3.36 msec, TR = 2300 msec) was acquired to provide high-resolution images.

VBT as applied to stroke cases

The VBT method applied to stroke subjects can be summarized in 4 sequential steps:

1) *Tissue preparation* (Fig. 1): the preliminary preparation of the brain images had three stages, aimed at obtaining a suitable representative image of the undamaged hemisphere, from which tissue analogous to the region could be reliably extracted.
   a) *Demarcation of the lesion boundaries*: demarcation of the lesion was performed manually (Fiez et al., 2000), and then temporarily marked by giving the relevant voxels an intensity value of 250 (using the AFNI command 3dcalc). This prevented loss of this area during creation of a skull stripped mask (Skull stripping was performed using AFNI's 3dSkullStrip utility). This step was visually checked and corrected if areas were missing or non-brain areas were included.
   b) *Sulcal marking*: several sulci were drawn by hand, slice by slice, in the original volume

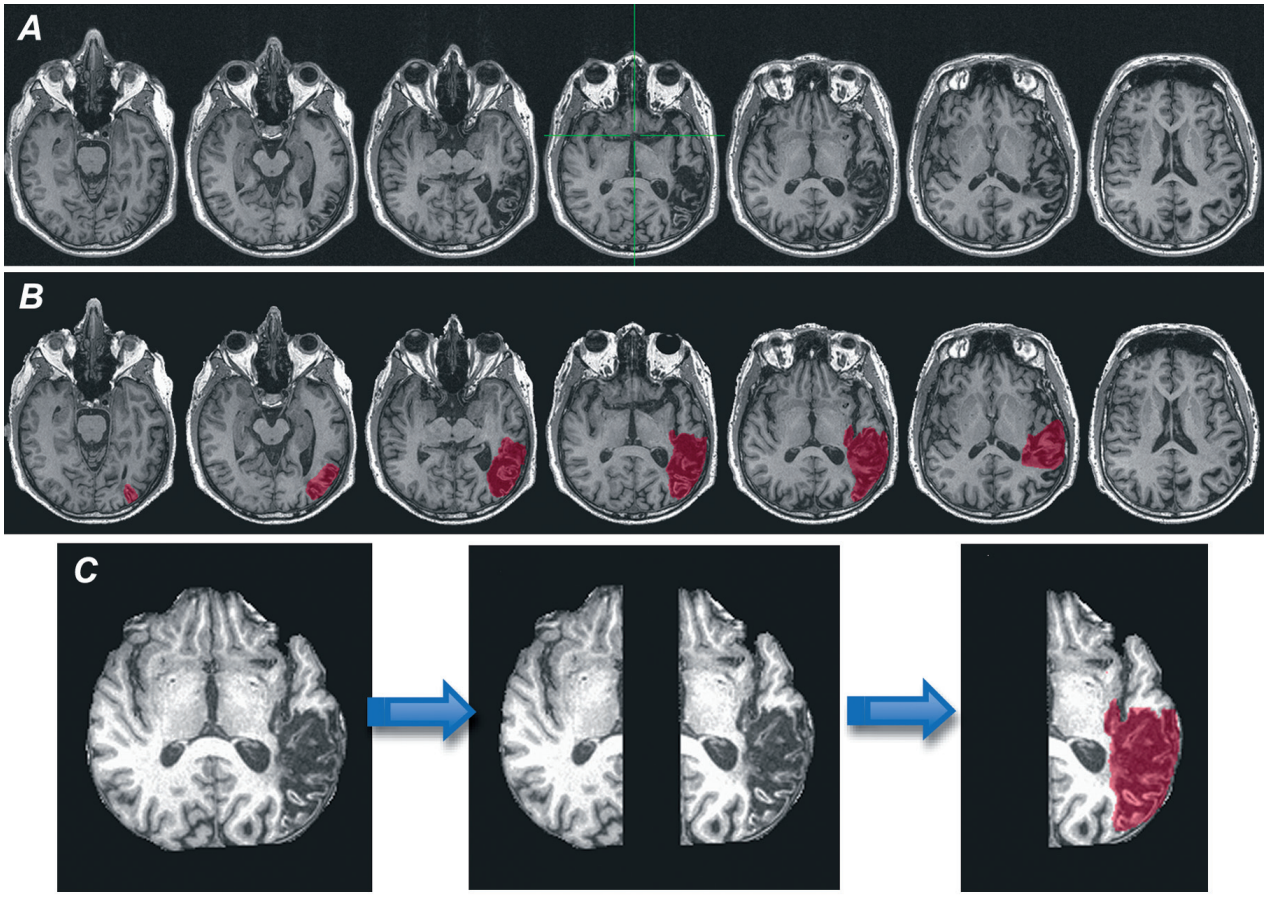

Fig. 1. - Tissue preparation. This figure illustrates the pre-processing done in order to obtain proper images to perform the virtual tissue transplantation as exemplified in an individual case. A) T1-weighted axial images showing the extent of the lesion in the MCA territory. B) Mask drawn by hand overlying the lesioned tissue. C) Axial sections showing the sequential steps for the segregation of the brain after the skull stripping and after the separation of the right and left hemispheres. The final panel shows the superimposition of the lesion mask on the stroke located in the left hemisphere.

space, in order to have anatomical guidance for the morphing steps described in the following section. These sulci were located in a variety of cortical regions to guarantee that all planes were represented. Because of the variance in the lesions, not all sulci were drawn (at this point) for all subjects. However after the VBT, the missing sulci within the lesion were then drawn as well. The following sulci were included: central sulcus (CS), collateral sulcus (colS), precentral sulcus (PreCS), transverse temporal sulcus (TTS), postcentral sulcus (PostCS), intraparietal sulcus (IPS), superior frontal sulcus (SFS), occipito parietal sulcus (ParOccS), inferior frontal sulcus (IFS), calcarine sulcus (calcS), superior temporal sulcus (STS), pericallosal sulcus (PCS), inferior temporal sulcus (ITS), anterior occipital sulcus (antOS) and Sylvian fissure (SF). Some of these are included in Caret (Van Essen and Dierker, 2007) and have been used in other studies for quantification of sulcal geometry (Toga et al., 2001). Because these sulci are drawn by hand, this step can be time consuming, especially for a naïve researcher.

c) *Hemispheric separation*: transplantation of the homologue requires producing a representative image of an undamaged hemisphere, from which tissue analogous to the region can be extracted. To produce this image, the hemispheres must undergo separation from each other and manipulation for alignment. This required two steps. a) Partitioning of the brain into right and left sides: To divide the volume into left and right hemispheres, we transformed the anatomical dataset to the TT_N27 Talaraich template (the "Colin" brain – one subject scanned 27 times and averaged, using the AFNI command @auto_tlrc, with a full affine (12 degrees of freedom) transformation). b) We then used this inverse transform to obtain the left hemisphere (positive x Talaraich coordinate) and right hemisphere (negative x Talaraich coordinate) in the original volume space. The end result of this procedure was two half brains: right without stroke and the left with the stroke.

2) *Dissection of the homologous non-stroke tissue* (Fig. 2): the goal of this step was to extract, from the right hemisphere, the homologous brain corresponding to the lesioned tissue from the left hemisphere. For this, first we created a mirror image of the non-stroke hemisphere by flipping it using the AFNI function 3dLRflip. Subsequently, we shifted the flipped right hemisphere to match the location of the left one, using a rigid affine transformation (6 degrees of freedom), guided by the relative location of the drawn sulci. At this point, particularly in cases with large lesions, the

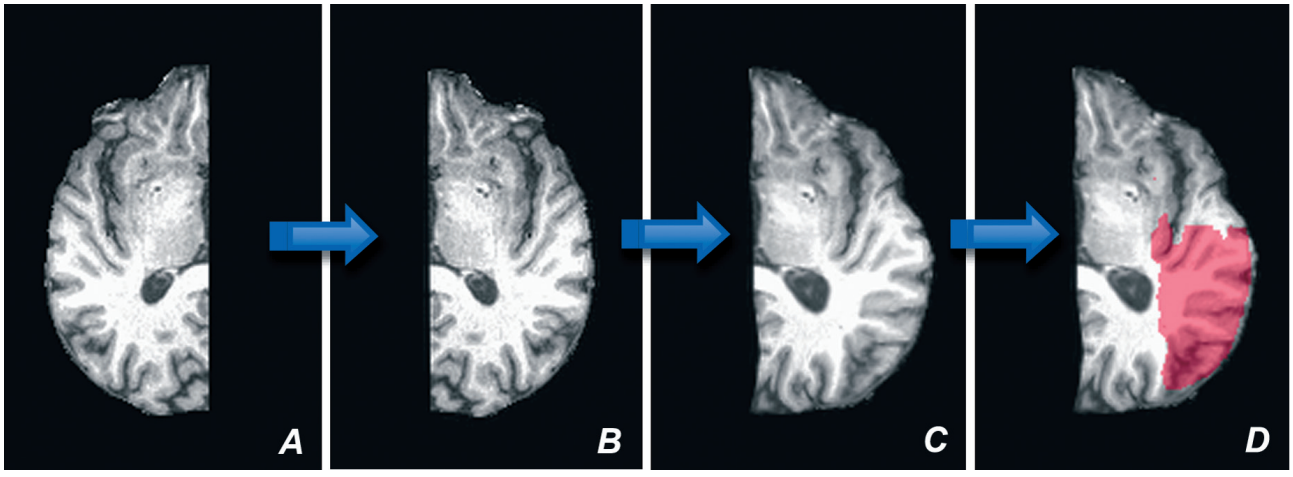

Fig. 2. - Dissection of the homologous non-stroke tissue. This figure summarizes the steps done on the right hemisphere in order to dissect healthy tissue homologous to the lesion present in the contralateral side. A) Initial stage is obtaining an image with the right side of the brain. B) The right brain is flipped and registered to the left side. C) Followed by resizing it to the size of the left hemisphere. D) Finally, the lesion mask can be superimposed to the flipped right hemisphere to obtain the tissue to be transplanted.

left hemisphere tended to be more atrophic than the right. The next step required a non-linear deformable warping of the right hemisphere to the left, guided by areas outside the lesion. This was done using the symmetric and diffeomorphic (smoothly invertible) non-linear warping algorithm SyN (Symmetric Normalization), along with a *Cost-function lesion mask* (an inverted version of our lesion mask), that is part of the ANTS package (Advanced Normalization Tools found at: http://www.picsl.upenn.edu/ANTS/references.php). While this program is commonly used to spatially normalize one subject to another or to a common template, here we applied it to spatially normalize the subject's contralesional hemisphere to side with the lesion. Thus this program allows warping the (already roughly aligned) right hemisphere to fit exactly the size of the left (lesioned) hemisphere, producing a more accurate transplant.

3) *Tissue transplantation* (Fig. 3): the goal of this step was to perform the transplantation and adjust it to replace the lesion produced by the stroke. In the initial step, an exact hand-drawn mask of the lesion was used to extract the selected VBT tissue, using AFNI's 3dcalc utility. This utility was then used to create a dataset in the *same space as the original*, but with virtual brain tissue transplanted into the lesion space. Like any tissue transplant, dropping in foreign tissue results in visible "scar" lines between the original and transplanted tissue. These lines are reduced by effectively "suturing" the two tissues together using morphing software, which retains the original anatomy of the lesioned brain, but reduces the stark contrast between the two tissues in the white and gray matter. A thin ribbon of tissue surrounding the original lesion was used to "suture" the new transplanted tissue to the original brain tissue. To create this thin ribbon, a slightly expanded lesion mask was used, which expanded the lesion by 2 mm on all sides. The expanded lesion mask was created by applying a kernel that took the mean of non-zero voxels within a 2 mm radius (AFNI 3dmerge) of the original lesion mask (which had only 1 and 0 values anyways). Then a dataset was created using the same methods as before containing a slightly larger, expanded VBT. 2D TIFF images were created of each dataset in the axial orientation. Images of the expanded VBT dataset and the original VBT dataset were morphed together using Xmorph (http://xmorph.sourceforge.net/) to create a new set of 2D images. The datasets are identical anatomically in every aspect except for a small region of tissue, allowing only this ribbon to be affected by the morphing program. Weighting the morphing algorithm towards the original VBT causes the ribbon to be more similar, anatomically, to the original tissue, while reducing contrast along the edge of the VBT by allowing gradual blending of the "suture" lines (Fig. 3A', B'). Though similar in appearance to the original, the ribbon of tissue has been altered from the original, and must be excluded in further analysis. To produce a 3D dataset from a 2D set of images, AFNI program to3d was used, with the flag-datum short selected.

   If the transplanted tissue still had small inhomogeneities after morphing in the borders between the transplantation and the surrounding brain, voxel intensities were made uniform using FSL's FAST (http://www.fmrib.ox.ac.uk/fsl/fast4/index.html), a program which performs bias field correction (as well as intensity-based segmentation). As a final touch, manual voxel corrections were made first on the segmented masks, if needed, as judged by visual inspection. Then, in the final transplant, voxels receiving these corrections were replaced by the average intensity value of other voxels that were part of the corresponding segmentation (white matter, gray matter or CSF), found within a sphere of 3 mm. (This was done using AFNI's 3dLocalStat and 3dcalc commands, along with the segmentation masks from FAST).

   The end result of this step was replacement of the original lesion by healthy tissue from the homologous contralateral side.

4) *Cortical surface registration and parcellation* (Fig. 4): next, using the new reconstructed brain, we used the Freesurfer software package (Dale et al., 1999; Fischl et al., 1999) to create surface representations of each participant's anatomy, by inflating each hemisphere of the anatomical volumes to a surface representation, and parcel-

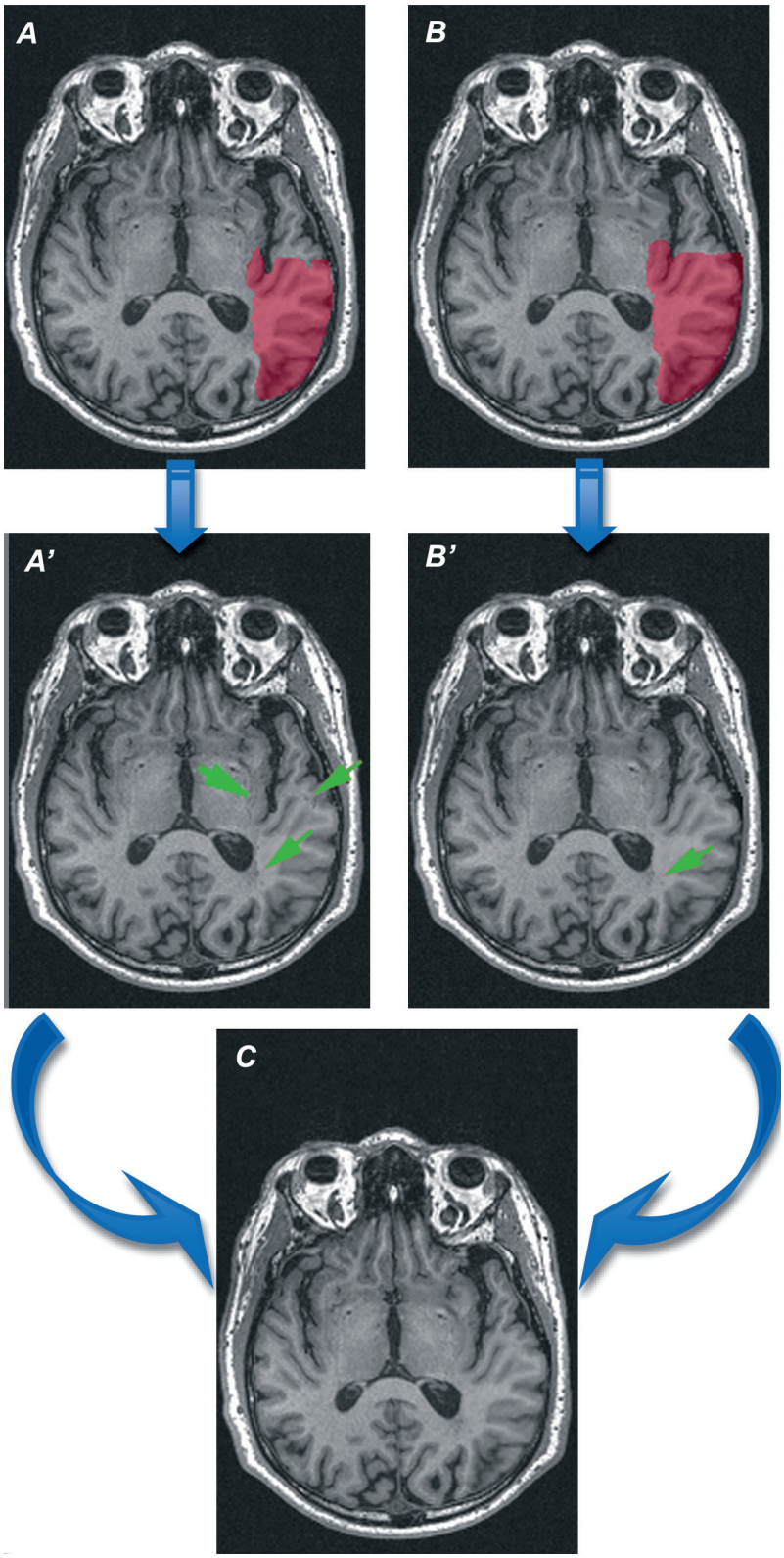

Fig. 3. - Tissue transplantation. This figure illustrates the warping of the transplant to the left hemisphere. A) Transplantation with the original lesion mask; B) Transplantation with the expanded lesion mask; A' and B') Arrows mark sites where the transition between the native tissue and the transplantation is not smooth; C) Final result from the iterative morphing process between these two transplants. Note that the transition areas are much more smooth and homogeneous.

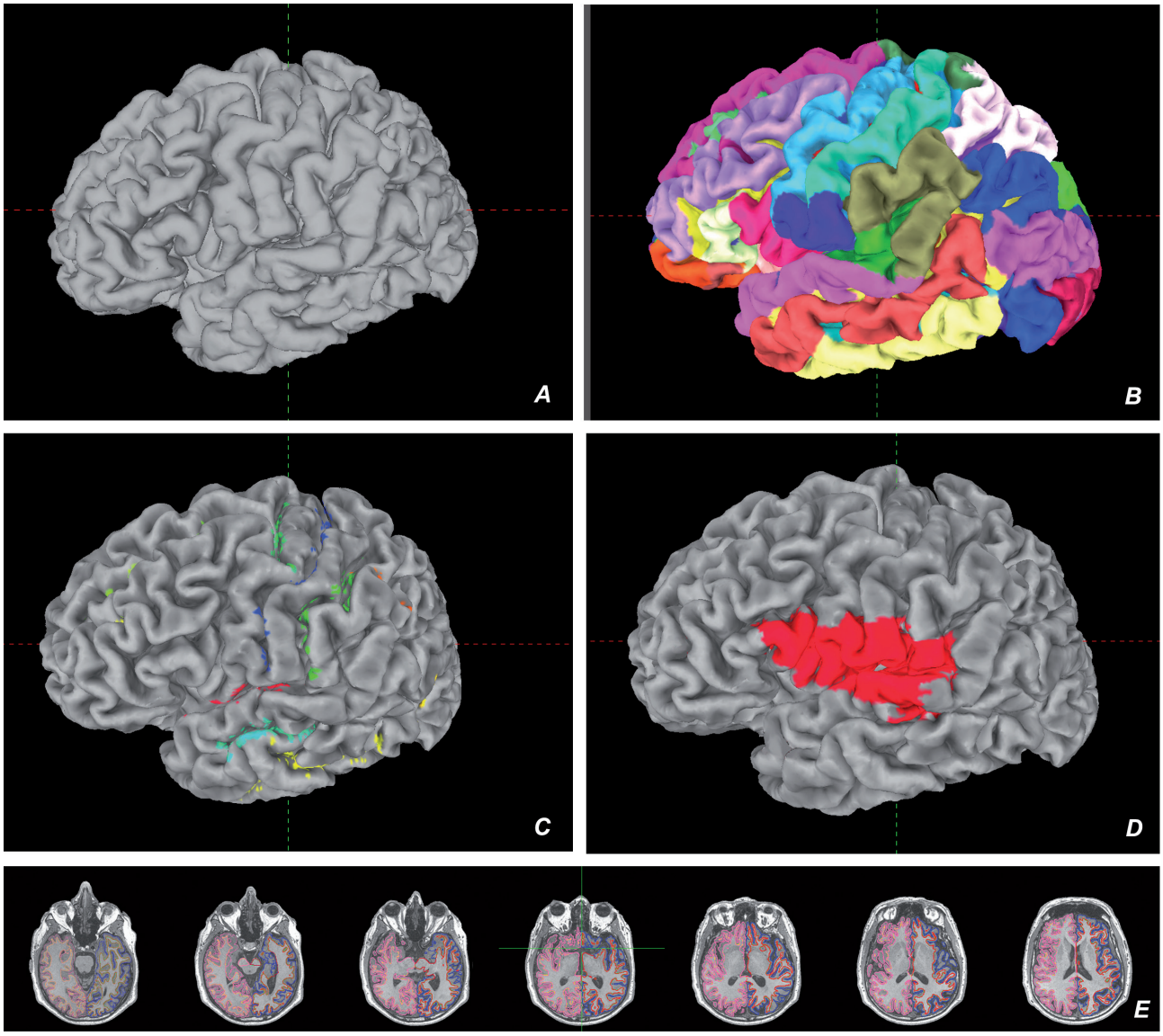

Fig. 4. - Cortical surface registration and parcellation: Figure depicting the anatomical reconstruction by Freesurfer from the reconstructed left hemisphere. A) Surface anatomy of the left hemisphere. These 3-D images were used for the gross anatomical assessment of the left hemispheres in each individual subject; B) Freesurfer parcellation scheme on the transplanted left hemisphere; C) Hand drawn sulci from the lateral brain represented in the 3-D Freesurfer reconstruction; D) Lesion mask as seen in the 3-D Fresurfer reconstruction; E) Freesurfer segmentation of white matter and gray matter in the reconstructed brain. These axial images at the level of the original stroke lesion were used for gross visual assessment of the quality of the segmentation.

lating this representation into regions with the Freesurfer's classification algorithm, based on the subject's anatomical values and prior probabilities from its 2005 Destrieux atlas (Fischl et al., 2004). SUMA (Saad et al., 2004) was then used to import the surface representations and project the cortical parcellation from the 2D surfaces back into the 3D volume in AFNI, as well as the sulcal landmarks and lesion drawn in the 3D volume to the 2D surface. The pipeline for the entire method is shown in Fig. 5.

VBT biological validation

The biological validation of our method was performed in two ways:

a) Visual inspection of the Freesurfer surface reconstruction was performed by two anatomists (RK, AS). The visualization of the gross anatomy

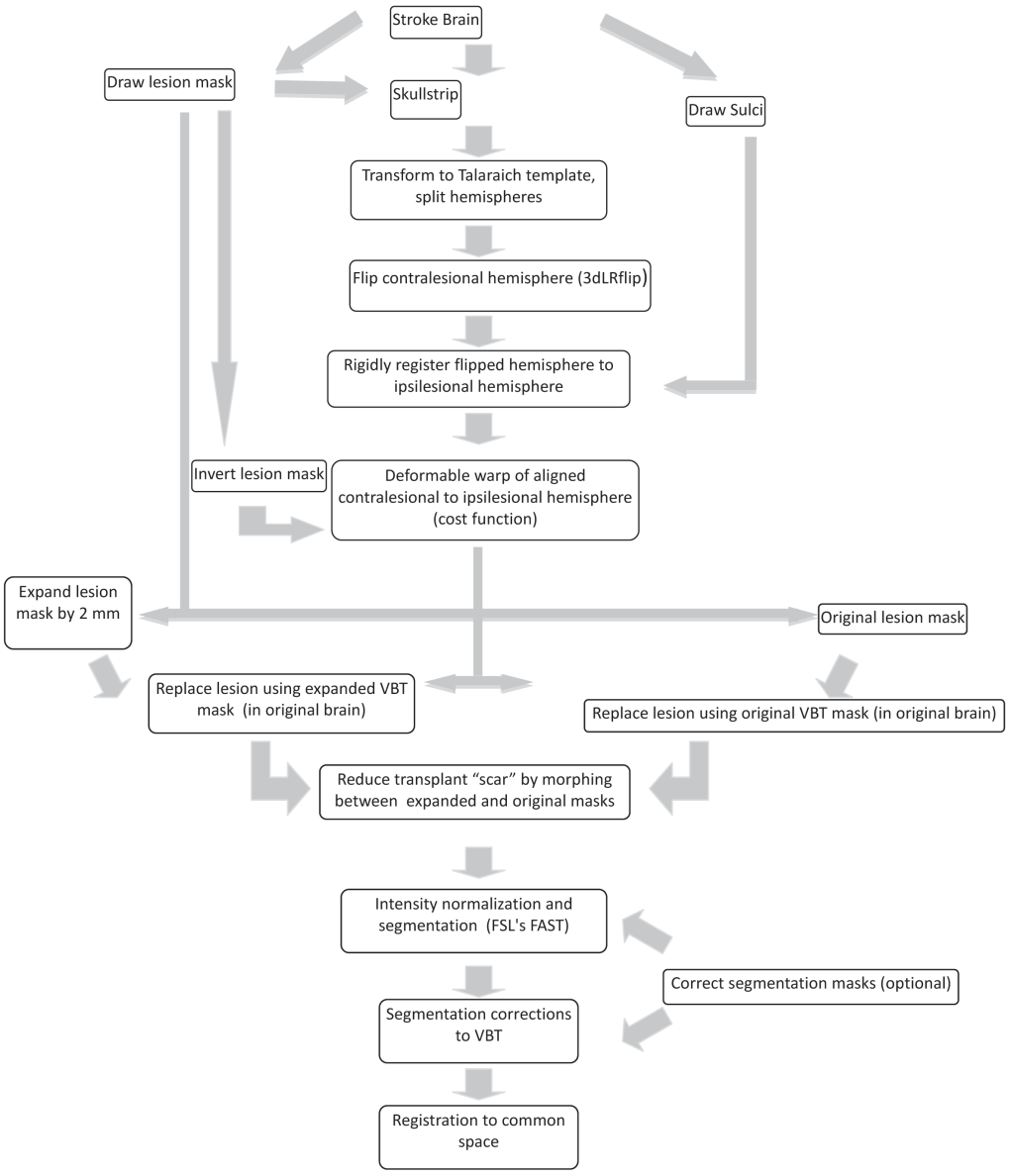

Fig. 5. - Pipeline showing the overview of the methods. Depiction on the sequential steps included in the VBT method. The only step not automatized is the manual drawing of the sulci. For details on the steps, please refer to the methods section.

of the cerebral cortex was performed in the 3-D reconstructed brains containing the drawn sulci (Fig. 4C). This provided a qualitative assessment of the location of the sulci and the general anatomy. In addition, visualization was conducted using AFNI to examine the location of the Freesurfer segmentation, as seen in the 2-D T-1 weighted images. The idea was to assess the smoothness of the transition between the native and transplanted tissue.

b) Quantitative evaluation was performed with assessment of the sulcal landmarks. For this, we first added the sulci missing due to the lesion but now included in the transplanted tissue. Based on the cortical surface registration and Freesurfer parcellation, we then used AFNI to compute the labels and number of voxels for each sulcal landmark. The average number of voxels under each labelled sub-region was obtained and categorized according to its location within or outside the

lesion. Thus, this quantitative "profile" refers to the number of Freesurfer regions crossed by the traced sulci.

Statistical analysis

The input data used was a "normalized number of voxels" defined as the average number of voxels across subjects in a Freesurfer region divided by the sum of all voxels in the corresponding brain region multiplied by 100. This was done for each ROI located within and outside of the lesions for each individual. The normalization was used because we were interested in testing differences between the hemispheres in the Freesurfer profiles rather than the number of voxels per subregion (within ROIs). Pearson's chi-squared test was then used to test whether there was a distribution difference between the left hemisphere and the right hemisphere for sulci that were located in the affected and unaffected brain regions.

Results

Pilot study

Internal comparison

To determine whether transferring homologous brain regions is better than transferring regions from a Talairach template, we ran both versions in the FreeSurfer pipeline and examined which one obtained results more similar to those seen in the original, non-lesioned brain. This analysis indicated that transferring homologous regions resulted in parcellation results highly similar to those found for the non-lesioned brain (median accuracy = 78%). In contrast, transferring regions on the basis of a Talairach template resulted in markedly different parcellation results and lower accuracy (median = 52%). The results of the internal comparison therefore showed that VBT of the homologue was the most accurate, and thus external comparison of the method was conducted using this type of tissue (Wier et al., 2006). This comparison can be seen in Fig. 6.

External comparison

To assess the amount of displacement introduced by the method and compare our alignment method to an alternative method, we aligned the VBT brains using either the FreeSurfer pipeline or Cost-function masking. The mean normalized overlap using the Freesurfer alignment was 65% ± 20 and for the Cost-function masking was 66% ± 16. The Wilcoxon signed rank test had a statistic value V = 32 and corresponding p value = 0.62 demonstrating no difference between the two methods.

Stroke study

Qualitative anatomical evaluation

The first step in the evaluation of the VBT method was visual inspection of the reconstructed brains by two anatomists (RK and AS). The inspection was

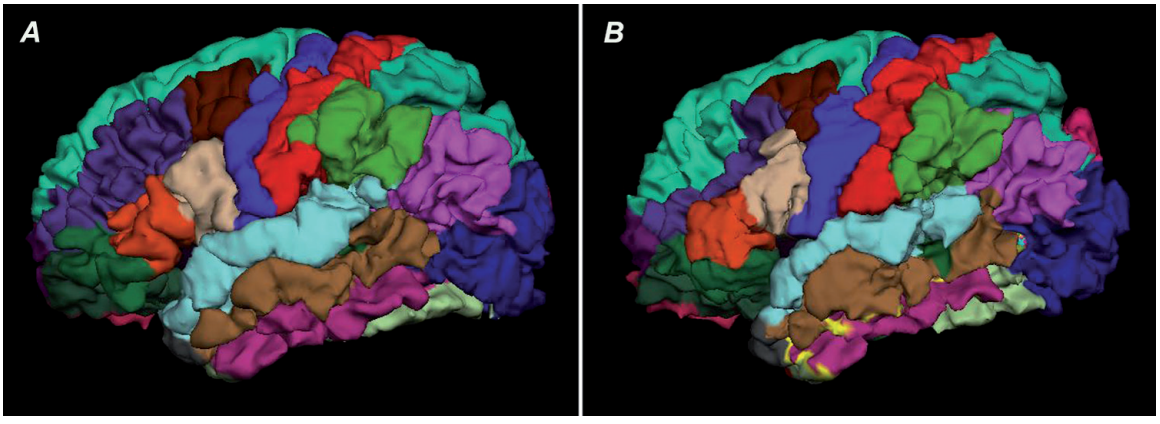

Fig. 6. - Freesurfer parcellations Comparing the Homologous and Tailariach transplantations. Accuracy of the homologous (A) and TTatlas (B) transplantations where assessed against a non-lesioned brain. The accuracy of registration was quantified by determining the extent of overlap between the location of the anatomical region and its location when registration was applied to the complete (non-lesioned) version of the brain in question. For each of the 12 brains, a Hits-FalseAlarms measure quantified the extent of accuracy. Note the anatomical inaccuracies of the Freesurfer parcellation when the transplantation was based on the TTatlas.

performed using two strategies. First was a visual inspection of the gross anatomy of the Freesurfer reconstructed 3-D individual brains. The sulcal landmarks were superimposed onto these reconstructions (Fig. 4) and inspected for proper placement. This visualization provided general coherence of the gross anatomy of these brains for each individual.

The second approach was visual inspection of 2-D images with the overlap of the Freesurfer segmentation. This was accomplished in individual sections as shown in Fig. 4. This procedure focused on the transition points between the transplanted and the surrounding, non-stroke tissue.

Cases with problems in either one of these inspections were reprocessed. In general, these reprocessed cases had a poorer gray matter-white matter definition due to either aging or low quality of the structural T1-weighted image.

Sulcal quantification

The sulcal Freesurfer profiles (volumes of different Freesurfer labeled regions crossed by each drawn sulci) were not constant across all sulci. Depending on the complexity of the particular sulcus, some had few Freesurfer region labels associated with them (e.g., pericallosal sulcus), whereas others had many more (e.g., calcarine sulcus).

Because of this variability, assessing the validity of the VBT methodology was performed in two ways: First, we examined the accuracy of the method by comparing the profiles for sulci outside the stroke in the left and right hemispheres, and second, we did this comparison in sulci that in some subjects were within the volume of the stroke and in others outside the stroke.

Table II summarizes these results that are also shown in Figs. 7, 8, 9 and 10.

The Freesurfer label profile of those sulci never affected by the stroke lesion (calcarine, collateral, pericallosal, anterior occipital, intraparietal and para-occipital) did not differ between the right and the left hemispheres (Fig. 7), i.e., their profiles were similar, independent of the number of voxels. A similar trend was observed in some sulci not affected in

Table II. - Summary of the Chi Square comparisons on the distribution of regional profiles for each ROI. They are classified according to their location inside or outside the lesion.

		Chi Square	df	p value
Sulci within lesion	Central	3.10	4	0.54
	Precentral	13.04	6	0.04
	Inferior Frontal	0.00	1	0.98
	Postcentral	0.27	1	0.60
	Superior Temporal	0.95	2	0.62
	Superior Frontal	0.53	2	0.77
	Sylvian Fissure	9.65	8	0.29
Sulci outside lesion	Calcarine	0.74	4	0.95
	Collateral	1.73	3	0.63
	Pericallosal	0.79	2	0.67
	Anterior Occipital	4.11	3	0.25
	Intraparietal	1.46	2	0.48
	Para-occipital	2.52	6	0.87
	Central	3.75	4	0.44
	Precentral	38.59	4	8.45E-08
	Postcentral	2.20	1	0.14
	Inferior Frontal	17.60	3	5.32E-04
	Superior Temporal	2.34	2	0.31
	Superior Frontal	2.02	2	0.36

df = degrees of freedom.

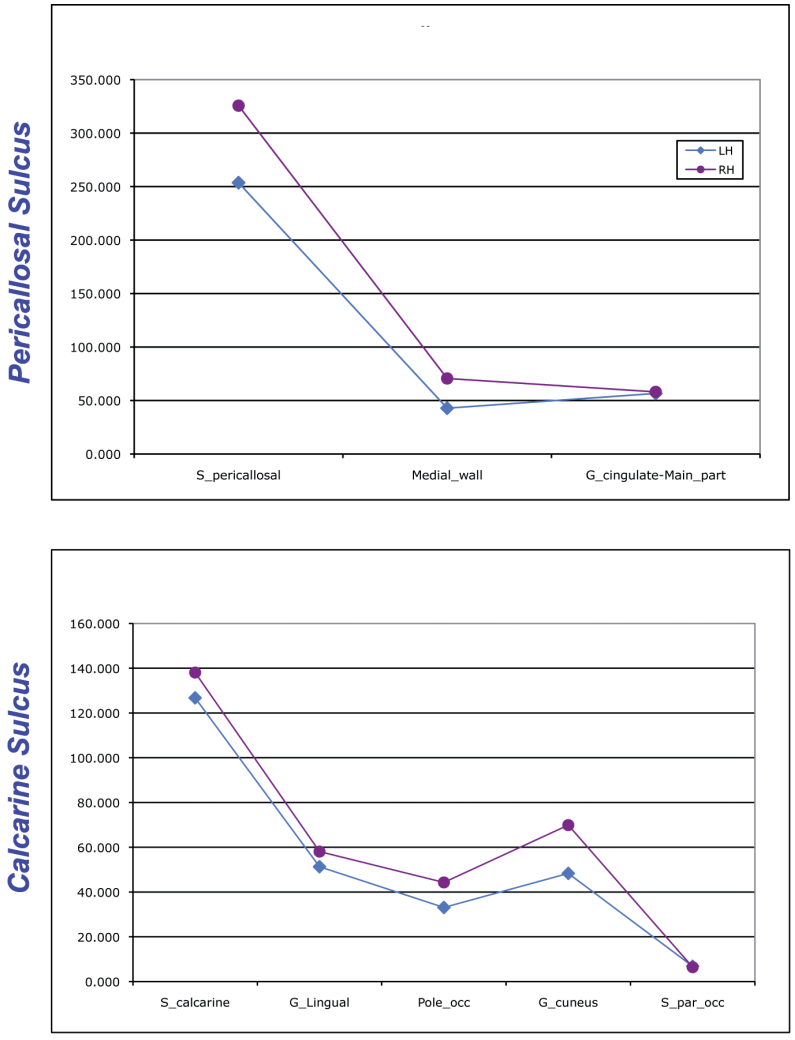

Fig. 7. - Sulci distribution outside the lesion. Comparison of average number of voxels from all subjects (Y axis) per Freesurfer labels (x axis) between the right and left hemispheres of two sulci (pericallosal and calcarine) that were never part of the lesion. Note the close correspondence in the patterns of labeling done by Freesurfer in both sulci. The Freesurfer profile for all sulci that were never affected by the lesion, were similar in the left and right hemispheres.

all subjects (central, postcentral, superior temporal, superior frontal; Fig. 8) as well as in the Sylvian fissure (Fig. 9), which was affected in all these aphasic subjects. In contrast, significant differences between hemispheres were seen in the precentral sulcus inside and outside the lesion and the inferior frontal sulcus outside the lesion (Fig. 10).

Independent of the contrast between hemispheres, all sulci (except the inferior frontal sulcus) showed similar inter-hemispheric trends when comparing sulci within and outside the lesion. By contrast, the inferior frontal sulcus did not follow the same pattern between the non-stroke hemisphere and the transplanted tissue. Whereas there inter-hemispheric differences were significant in the non-stroke cases, in the cases where the transplant included this sulcus, there were no inter-hemispheric differences. In addition, the complexity of the transplanted sulcus was reduced in comparison to the non-transplanted side (Fig. 10).

Describing and quantifying the lesion (Table III)

The main objective for developing VBT was to use automatized brain parcellation schemes in MRI T1-weighted images in patients with large cortical strokes in order to ascertain the location of activation with fMRI. However at the same time, it was also

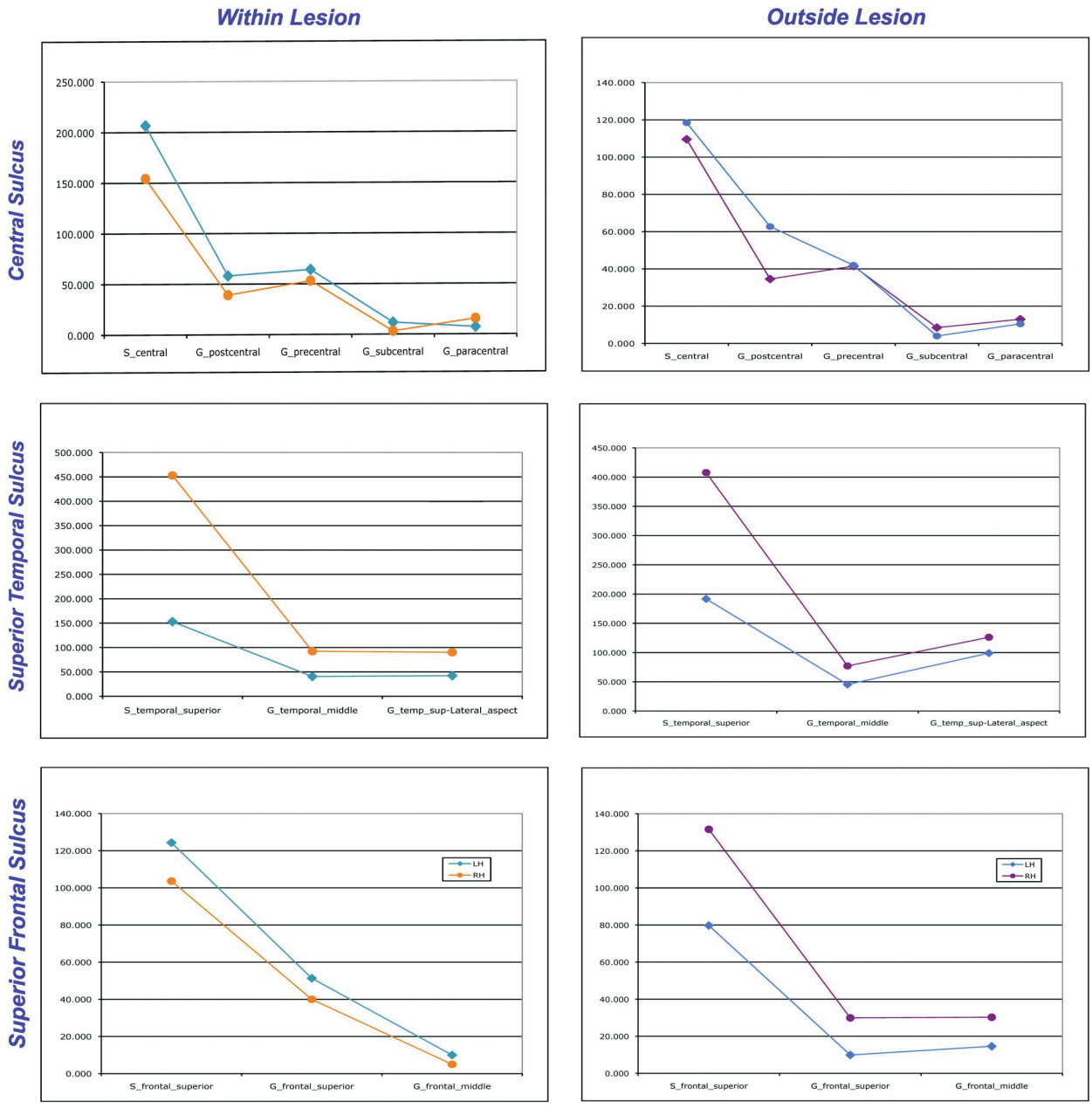

Fig. 8. - Comparison of sulci distribution within and outside the lesion: Comparison of average number of voxels from all subjects (Y axis) per Freesurfer labels (x axis) between the right and left hemispheres of sulci that were affected by the stroke in some cases (left column) but not in others (right column). Note the close correspondence on the Freesurfer profiles in the reconstructed cases when compared to those in intact cases. The only exception to this being the inferior frontal sulcus which had a more simple distribution in the reconstructed cases.

possible to obtain the anatomical description within the lesion mask as described with the Freesurfer parcellation. Table III lists the Freesurfer labeled regions included in the lesion in subject #6. In this particular instance, we know the total number of voxels in each region, and thus we were able to calculate the percent of the each region affected by the stroke. This computation is quite informative since it shows a more precise location of the lesion with its burden on each region. In this particular instance, the subcentral sulcus and gyrus were essentially destroyed by the stroke. This region corresponds to Brodmann's area 43 and includes opercular regions within the Sylvian fissure, including the pre and

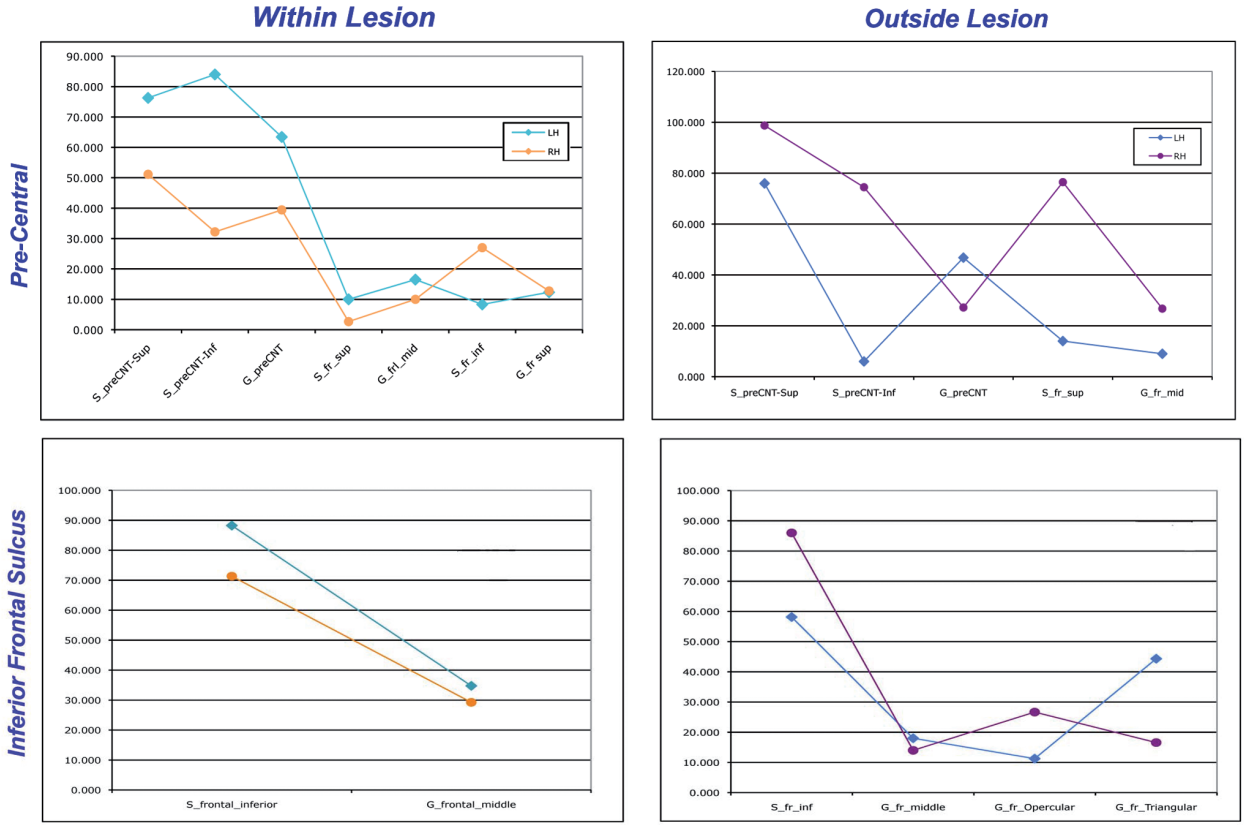

Fig. 9. - Distribution of Sylvian fissure within the lesion: Comparison of average number of voxels from all subjects (Y axis) per Freesurfer labels (x axis) between the right and left hemispheres in the Sylvian fissure which was affected by the stroke in all participants. Note the close parallels between the Freesurfer profile in the right and left hemispheres.

post-central gyri extending to the anterior portion of the supramarginal area posteriorly and with the insular cortex medially. Other regions heavily affected were the planum temporale, the opercular portion of the inferior frontal gyrus and the anterior vertical ramus of the Sylvian fissure. In contrast, even when a large number of voxels in the cortical white matter was affected (16546), this constitutes a relatively small fraction of this region (7.3%).

Discussion

The present manuscript describes a reliable method for registration and parcellation of brains with large cortical strokes. This work is based on the original report by C. Weiller, who suggested "filling in" the lesion with normal tissue (Weiller et al., 1995), and a more recent report implementing that idea using simulated lesions on normal brains (Nachev et al., 2008). In contrast, the present work expands on these previous efforts by not only applying the reconstructed brains to surface brain parcellation schemes, but more importantly, by implementing and applying the method to brains with large lesions produced by ischemic strokes.

Because automatic registration software requires structural (not necessarily morphological) integrity of brain tissue, our method replaces the structural loss of tissue by contralateral brain not directly affected by the stroke.

If one considers the degree of asymmetry between hemispheres, this notion may represent an oversimplification. Indeed, the literature is laden with examples of the anatomical differences between the cortical hemispheres. Differences are evident not only in the volumes of individual brain regions (Hutsler et al., 1998; Watkins et al., 2001), but also in morphology, particularly sulcal morphology (Rademacher et al., 1993; Thompson et al., 1996; Zilles et al., 1997; Germann et al., 2005). The importance of this cortical asymmetry has been highlighted since at least

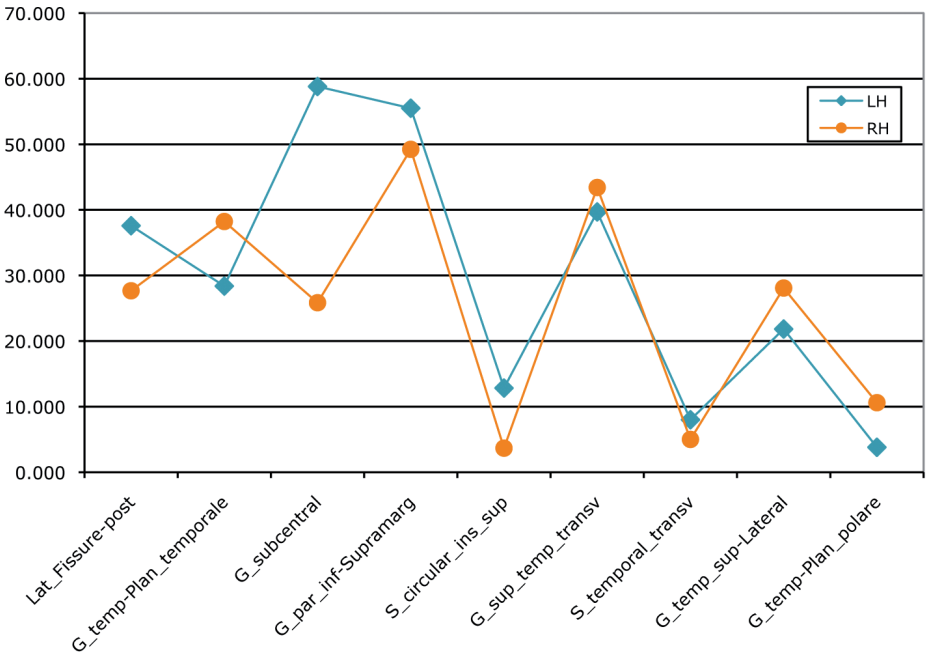

Fig. 10. - The case of frontal sulci: Comparison of average number of voxels from all subjects (Y axis) per freesurfer classifications (x axis) between the right and left hemispheres in the inferior frontal and the precentral sulci. The left column represent the cases affected by the stroke, the right column, the same sulci when not lesioned. Note the reciprocal relationship in the complexity of these sulci which tend to be some of the most variable in the brain.

Broca (1861) as a means to support lateralization of function (Broca, 1861) and etiology of pathology (see Watkins et al., 2001). On the other hand, although interhemispheric anatomical asymmetry is clear, it is also clear that this anatomical variance between hemispheres is smaller than that anatomical variance of hemispheres among different individuals (Rademacher et al., 1993; Paus et al., 1996; White et al., 1997a, 1997b). Hence, it is reasonable to suggest that the use of the homologous contralateral hemisphere to replace the structural lesion is a better alternative than its replacement with other tissue. Furthermore, using the contralateral side also reduces potential variability from gender differences (Paus et al., 1996; Zilles et al., 1997).

That said, it is also evident that any method seeking to replace the lesion by non-damaged brain needs to take into consideration the nature of the anatomical variability across hemispheres, even within an individual. With respect to VBT, we performed two different types of validation: computational and biological. The computational validation targeted the ideal computational methods to obtain the best possible registration parameters for a common anatomical space. The anatomical validation sought to assess the registration in terms of its biological consistency and reproducibility.

Computational validity (internal and external comparisons)

The results of the internal and external comparisons showed that the VBT of the homologous tissue is reasonably accurate, demonstrated by the overlap between the non-lesioned brain and the homologous VBT (Wier et al., 2006). However, it was also evident that occasionally the method leads to false positive parcellations. Because of this limitation, we improved the previous method by increasing the accuracy of the registration between the non-stroke and the stroke hemispheres. This was achieved by means of a non-linear warping guided by the locations of sulci identified a priori.

Biological validity

Assessing biological validity required testing the method in individuals with large cortical lesions produced by ischemic stroke. This is important because the anatomical variance between the hemispheres is affected not only by the natural differences between them as described above, but also by the

Table III. - Example of regional classification of the lesion by Freesufer in an individual subject. The burden of the lesion refers to the percent of the total region affected by the lesion.

Freesurfer Anatomical Region	Number of Voxels	Burden of lesion per region (%)
G_frontal_inf-Opercular_part	1412	41.8
G_frontal_inf-Triangular_part	33	1.5
G_frontal_middle	247	2.2
G_insular_long	13	1.5
G_occipit-temp_lat-Or_fusiform	95	2.3
G_parietal_inferior-Supramarginal_part	724	11.2
G_postcentral	36	0.9
G_precentral	248	3.7
G_subcentral	2494	87.1
G_temporal_middle	54	0.6
G_temp_sup-G_temp_transv_and_interm_S	297	30.4
G_temp_sup-Lateral_aspect	1462	25.3
G_temp_sup-Planum_polare	26	1.7
G_temp_sup-Planum_tempolare	2102	70.1
Lat_Fissure-ant_sgt-ramus_vertical	274	40.4
Lat_Fissure-post_sgt	486	33.9
S_central	283	5.7
S_cingulate-Main_part_and_Intracingulate	103	1.5
S_circular_insula_inferior	70	2.7
S_circular_insula_superior	391	12.7
S_frontal_inferior	107	3.7
S_frontal_middle	21	0.5
S_frontomarginal	25	2.2
S_intermedius_primus-Jensen	1	0.2
S_occipital_anterior	6	0.3
S_occipito-temporal_lateral	195	15.0
S_occipito-temporal_medial_and_S_Lingual	427	13.3
S_precentral-Inferior-part	886	29.8
S_subcentral_ant	143	100.0
S_subcentral_post	314	99.4
S_temporal_inferior	47	1.8
S_temporal_superior	2184	26.7
S_temporal_transverse	318	97.8
Cerebral white matter	16546	7.3

G = gyrus; S = sulcus.

atrophy and mechanical deformation produced by the stroke (Bucy, 1964; Warabi et al., 1990; Graham and Landtos, 2002; Kabir et al., 2007). Additional sources of variance come from the contralesional hemisphere itself because it too can be affected by the stroke, both functionally and anatomically, by secondary atrophy and diaschisis (Slater et al., 1977; Reggia et al., 2001; Kraemer et al., 2004; Lotze et al., 2006; Schaechter et al., 2009). Under these circumstances, it is essential to quantify appropriate controls for the registration of the tissues.

Sulcal variance outside the lesion

Because the original goal was to obtain proper registration and parcellation of the ipsilesional tissue not affected by the stroke (allowing the proper alloca-

tion of fMRI activation in the anatomical space), the first validation should demonstrate accurate parcellation of this tissue.

Indeed, our results did not find statistical differences in the profiles of the Freesurfer regions between the two cortical hemispheres. In other words, the resulting parcellation for both hemispheres was similar, supporting the assumption of a proper anatomical classification after VBT in the ipsilesional hemisphere. This included the absence of misclassified regions. On the other hand, the fact that the parcellation was similar in both hemispheres is somewhat surprising since the variance of some of the sulci included in this group (e.g., collateral and intraparietal) across individuals (Pruessner et al., 2002; Choi et al., 2006; Swisher et al., 2007) is larger than the variance for others (calcarine, pericallosal, anterior occipital and parieto-occipital) (Gilissen and Zilles, 1996; Thompson et al., 1996; Malikovic et al., 2007). A possible explanation for this possibly unusual observation lies in the fact that the collateral and the intraparietal sulci were not drawn in their entirety, since their original use was to guide tissue registration. Consequently, our results do not rely on full identification of the sulci, and thus these particular results on inter-hemispheric variability should be taken with caution.

Despite the similarity in how Freesurfer labeled the regions for these "intact" sulci in the two hemispheres, slight differences in the number of voxels between the hemispheres were noted in the pericallosal, the anterior-occipital, the intraparietal and the collateral sulci. In each of these cases, the number of voxels in several Freesurfer regions within each ROI tended to be larger in the (uninjured) right hemisphere compared to the (injured) left hemisphere. The cause of this discrepancy cannot be determined, since it could be due either to functional lateralization biased to the right side (Eidelberg and Galaburda, 1984; Rademacher et al., 1993; Thompson et al., 1996; Zilles et al., 1997; Pruessner et al., 2002; Germann et al., 2005) or to larger atrophy of the left (ipsilesional) side.

Sulcal variance within the lesion

We also quantified the Freesurfer region profiles of those sulci affected by the stroke in some but not all individuals, and the Sylvian fissure, a region affected in all individuals in our cohort.

In the former group, as in the case of the ipsilesional tissue outside the lesion, almost all sulci were similarly classified by the Freesurfer parcellation in the right and left hemispheres. These sulci included the central, superior temporal and superior frontal, postcentral and the precentral sulcus. By contrast, the precentral sulcus showed significant interhemispheric differences (both within and outside the lesion). There were no mislabels in the ipsilesional hemisphere after VBT. With one exception noted below, the Freesurfer parcellation was similar independent of lesion for all sulci. These results reinforce the notion of the VBT as a reliable tool for anatomical parcellation of stroke cases. As before, in some sulci (superior temporal, inferior frontal and superior frontal), both within and outside the lesion, the right hemisphere had a larger number of voxels in one of the Freesurfer regions. This tendency was more pronounced for sulci outside the lesion compared to sulci within the lesion. These results may seem counterintuitive since these sulci are those that have been considered "language related regions" and lateralization to the left would be expected (Small and Hoffman, 1994; Binder et al., 1995; Beaton, 1997). On the other hand, because all our subjects had strokes, secondary atrophy is a highly likely factor behind the differences.

As mentioned, there was one ROI where we found a different region labeling profile between the right and left hemispheres when comparing sulci within and outside the lesion: the inferior frontal sulcus. Whereas outside the lesion, the Freesurfer profiles for the right and left hemispheres were statistically different, this was not so within the lesion. The reason for the interhemispheric difference outside the lesion is that in few subjects, there were more regions included in the contralesional hemisphere than the ipsilesional hemisphere. That is to say, the profile for the inferior frontal sulcus in the VBT hemisphere was less complex than for the contralesional hemisphere. In contrast, the inferior portion of the pre-central sulcus demonstrated the opposite tendency, with larger complexity within the lesion than outside. This mirror situation may not be of surprise, since they are both interconnected in a complex fashion, and the anatomical variance of this interconnection is very large (Germann et al., 2005; Juch et al., 2005; Schmitt et al., 2005; Keller et al., 2009).

Lastly, we turn to the Sylvian fissure, a particularly interesting region that was affected by the lesion in all our patients. In this case, we did not find a significant difference between the hemispheres. However, the asymmetry of volume and topology of the Sylvian fissure has been widely reported (Rubens et al., 1976; Steinmetz et al., 1990; Aboitiz et al., 1992; Jancke et al., 1994; Steinmetz, 1996; Foundas et al., 1999; Sowell et al., 2002; Keller et al., 2007). The emphasis has been given to volume rather than topology and has been used as basis for lateralization of language, especially in the posterior portion of the fissure and the parietal operculum. However, our statistical assessment did not focus on volumetric assessment but on anatomical profiles. These results point to the resilience of our method since the parcellation scheme was similar in both hemispheres even when subjects had lesions affecting a variety of sectors within the fissure.

Lesion quantification

Precise anatomical description of brain lesions has been sought for experimental lesions in macaques (Darling et al., 2009) and for stroke in humans (Mehta et al., 2003; Alexander and Stuss, 2006; Rudrauf et al., 2008), where the anatomical quantification of lesions can be rather limited.

Because of the anatomical reliability of our method and the fact that we parcellate the whole cortical mantle, an additional advantage of our parcellation is that we can obtain a much more precise metric on the extent of the lesion. Furthermore, because we parcellate the entire cortical mantle, we can also normalize the size of the lesion with different variables. In this particular work, we elected to show the percent of the total Freesurfer region affected by the stroke. An individual example is shown in the results section. This normalization provided us with the burden of the lesion, thus demonstrating the degree to which each region was directly affected by the stroke.

This detailed anatomical definition of the lesion in cortical stroke opens up the opportunity for new types of analysis. Not only can it be used as a covariant for further analysis, but by knowing the burden of lesion in each anatomical region, we can for the first time use that information to develop more accurate connectivity models that specify precisely the inputs and outputs considered in the models.

Acknowledgments

We want to thank Helen Wier and Jeremy Skipper for assisting in the initial analysis. The work was partly supported by the James McDonnell Foundation (Brain Network Recovery Group), and by the National Institutes of Health under grants RO1-NS54942 (AS), NIH R01-DC07488 (SLS), and R33-DC008638 (SLS).

References

Aboitiz F., Scheibel A.B., Zaidel E. Morphometry of the Sylvian fissure and the corpus callosum, with emphasis on sex differences. *Brain*, **115** (Pt 5):1521-1541, 1992.

Aharonov R., Segev L., Meilijson I., Ruppin E. Localization of function via lesion analysis. Neural Comput., **15**: 885-913, 2003.

Alexander M. and Stuss D.T. Frontal injury: impairments of fundamental processes lead to functional consequences. *J. Int. Neuropsychol. Soc.*, **12**: 192-193, 2006.

Arnold M., Halpern M., Meier N., Fischer U., Haefeli T., Kappeler L., Brekenfeld C., Mattle H.P., Nedeltchev K. Age-dependent differences in demographics, risk factors, co-morbidity, etiology, management, and clinical outcome of acute ischemic stroke. *J. Neurol.*, **255**: 1503-1507, 2008.

Beaton A.A. The relation of planum temporale asymmetry and morphology of the corpus callosum to handedness, gender, and dyslexia: a review of the evidence. *Brain Lang.*, **60**: 255-322, 1997.

Beaulieu A. A space for measuring mind and brain: interdisciplinarity and digital tools in the development of brain mapping and functional imaging, 1980-1990. *Brain Cogn.*, **49**: 13-33, 2002.

Binder J.R., Rao S.M., Hammeke T.A., Frost J.A., Bandettini P.A., Jesmanowicz A., Hyde J.S. Lateralized human brain language systems demonstrated by task subtraction functional magnetic resonance imaging. *Arch. Neurol.*, **52**: 593-601, 1995.

Biswal B.B., Mennes M., Zuo X.N., Gohel S., Kelly C., Smith S.M., Beckmann C.F., Adelstein J.S., Buckner R.L., Colcombe S., Dogonowski A.M., Ernst M., Fair D., Hampson M., Hoptman M.J., Hyde J.S., Kiviniemi V.J., Kotter R., Li S.J., Lin C.P., Lowe M.J., Mackay C., Madden D.J., Madsen K.H., Margulies D.S., Mayberg H.S., McMahon K., Monk C.S., Mostofsky S.H., Nagel B.J., Pekar

J.J., Peltier S.J., Petersen S.E., Riedl V., Rombouts S.A., Rypma B., Schlaggar B.L., Schmidt S., Seidler R.D., Siegle G.J., Sorg C., Teng G.J., Veijola J., Villringer A., Walter M., Wang L., Weng X.C., Whitfield-Gabrieli S., Williamson P., Windischberger C., Zang Y.F., Zhang H.Y., Castellanos F.X., Milham M.P. Toward discovery science of human brain function. *Proc. Natl. Acad. Sci. U.S.A.*, **107**: 4734-4739, 2010.

Broca P. Remarques sur le siege de la faculte du language articule, suivives d'une observation d'aphemie (perte de la parole). *Bulletines de la Societe Anatomique*, **36**: 330-357, 1861.

Bucy P.C. The central neural mechanism controlling movement, with special reference to the pyramidal tract. *Acta Neurochir. (Wien)*, **11**: 731-738, 1964.

Chiavaras M.M., LeGoualher G., Evans A., Petrides M. Three-dimensional probabilistic atlas of the human orbitofrontal sulci in standardized stereotaxic space. *Neuroimage*, **13**: 479-496, 2001.

Choi H.J., Zilles K., Mohlberg H., Schleicher A., Fink G.R., Armstrong E., Amunts K. Cytoarchitectonic identification and probabilistic mapping of two distinct areas within the anterior ventral bank of the human intraparietal sulcus. *J. Comp. Neurol.*, **495**: 53-69, 2006.

Crinion J., Ashburner J., Leff A., Brett M., Price C., Friston K. Spatial normalization of lesioned brains: performance evaluation and impact on fMRI analyses. *Neuroimage*, **37**: 866-875, 2007.

Dale A.M., Fischl B., Sereno M.I. Cortical surface-based analysis. I. Segmentation and surface reconstruction. *Neuroimage*, **9**: 179-194, 1999.

Damasio H. *Brain anatomy in computerized images*. 2nd Edition. New York, Oxford University Press, 2005.

Darling W.G., Pizzimenti M.A., Rotella D.L., Peterson C.R., Hynes S.M., Ge J., Solon K., McNeal D.W., Stilwell-Morecraft K.S., Morecraft R.J. Volumetric effects of motor cortex injury on recovery of dexterous movements. *Exp. Neurol.*, **220**: 90-108, 2009.

Dinov I.D., Mega M.S., Thompson P.M., Lee L., Woods R.P., Holmes C.J., Sumners D.W., Toga A.W. Analyzing functional brain images in a probabilistic atlas: a validation of subvolume thresholding. *J. Comput. Assist. Tomogr.*, **24**: 128-138, 2000.

Eidelberg D. and Galaburda A.M. Inferior parietal lobule. Divergent architectonic asymmetries in the human brain. *Arch. Neurol.*, **41**: 843-852, 1984.

Fiez J.A., Damasio H., Grabowski T.J. Lesion segmentation and manual warping to a reference brain: intra- and interobserver reliability. *Hum. Brain Mapp.*, **9**: 192-211, 2000.

Fischl B., Sereno M.I., Dale A.M. Cortical surface-based analysis. II: Inflation, flattening, and a surface-based coordinate system. *Neuroimage*, **9**: 195-207, 1999.

Fischl B., van der Kouwe A., Destrieux C., Halgren E., Segonne F., Salat D.H., Busa E., Seidman L.J., Goldstein J., Kennedy D., Caviness V., Makris N., Rosen B., Dale A.M. Automatically parcellating the human cerebral cortex. *Cereb. Cortex*, **14**: 11-22, 2004.

Foundas A.L., Faulhaber J.R., Kulynych J.J., Browning C.A., Weinberger D.R. Hemispheric and sex-linked differences in Sylvian fissure morphology: a quantitative approach using volumetric magnetic resonance imaging. Neuropsychiatry. *Neuropsychol. Behav. Neurol.*, **12**: 1-10, 1999.

Germann J., Robbins S., Halsband U., Petrides M. Precentral sulcal complex of the human brain: morphology and statistical probability maps. *J. Comp. Neurol.*, **493**: 334-356, 2005.

Gilissen E. and Zilles K. The calcarine sulcus as an estimate of the total volume of human striate cortex: a morphometric study of reliability and intersubject variability. *J. Hirnforsch.*, **37**: 57-66, 1996.

Gjedde A. Functional brain imaging celebrates 30th anniversary. *Acta Neurol. Scand.*, **117**: 219-223, 2008.

Goebel R., Esposito F., Formisano E. Analysis of functional image analysis contest (FIAC) data with brainvoyager QX: From single-subject to cortically aligned group general linear model analysis and self-organizing group independent component analysis. *Hum. Brain Mapp.*, **27**: 392-401, 2006.

Goense J.B. and Logothetis N.K. Neurophysiology of the BOLD fMRI signal in awake monkeys. *Curr. Biol.*, **18**: 631-640, 2008.

Gonoi W., Abe O., Yamasue H., Yamada H., Masutani Y., Takao H., Kasai K., Aoki S., Ohtomo K. Age-related changes in regional brain volume evaluated by atlas-based method. Neuroradiology, **52**: 865-873. 2009.

Graham D.I. and Landtos P.I. *Greenfield's Neuropathology*. New York, Oxford University Press, 2002.

Hennig J., Speck O., Koch M.A., Weiller C. Functional magnetic resonance imaging: a review of methodological aspects and clinical applications. *J. Magn. Reson. Imaging*, **18**: 1-15, 2003.

Hutsler J.J., Loftus W.C., Gazzaniga M.S. Individual variation of cortical surface area asymmetries. *Cereb. Cortex*, **8**: 11-17, 1998.

Jancke L., Schlaug G., Huang Y., Steinmetz H. Asymmetry of the planum parietale. *Neuroreport*, **5**: 1161-1163, 1994.

Juch H., Zimine I., Seghier M.L., Lazeyras F., Fasel J.H. Anatomical variability of the lateral frontal lobe surface: implication for intersubject variability in language neuroimaging. *Neuroimage*, **24**: 504-514, 2005.

Kabir Y., Dojat M., Scherrer B., Forbes F., Garbay C. Multimodal MRI segmentation of ischemic stroke lesions. *Conf. Proc. IEEE Eng. Med. Biol. Soc.*: 1595-1598, 2007.

Keller S.S., Highley J.R., Garcia-Finana M., Sluming V., Rezaie R., Roberts N. Sulcal variability, stereological measurement and asymmetry of Broca's area on MR images. *J. Anat.*, **211**: 534-555, 2007.

Keller S.S., Roberts N., Hopkins W. A comparative magnetic resonance imaging study of the anatomy, variability, and asymmetry of Broca's area in the human and chimpanzee brain. *J. Neurosci.*, **29**: 14607-14616, 2009.

Kennedy D.N. Making connections in the connectome era. *Neuroinformatics*, **8**: 61-62, 2010.

Kotter R., Sommer F.T. Global relationship between anatomical connectivity and activity propagation in the cerebral cortex. *Philos. Trans. R. Soc. Lond. B. Biol. Sci.*, **355**: 127-134, 2000.

Kraemer M., Schormann T., Hagemann G., Qi B., Witte O.W., Seitz R.J. Delayed shrinkage of the brain after ischemic stroke: preliminary observations with voxel-guided morphometry. *J. Neuroimaging*, **14**: 265-272, 2004.

Le Goualher G., Procyk E., Collins D.L., Venugopal R., Barillot C., Evans A.C. Automated extraction and variability analysis of sulcal neuroanatomy. *IEEE Trans. Med. Imaging*, **18**: 206-217, 1999.

Lotze M., Markert J., Sauseng P., Hoppe J., Plewnia C., Gerloff C. The role of multiple contralesional motor areas for complex hand movements after internal capsular lesion. *J. Neurosci.*, **26**: 6096-6102, 2006.

Malikovic A., Amunts K., Schleicher A., Mohlberg H., Eickhoff S.B., Wilms M., Palomero-Gallagher N., Armstrong E., Zilles K. Cytoarchitectonic analysis of the human extrastriate cortex in the region of V5/MT+: a probabilistic, stereotaxic map of area hOc5. *Cereb. Cortex*, **17**: 562-574, 2007.

Marcar V.L. and Loenneker T. The BOLD response: a new look at an old riddle. *Neuroreport*, **15**: 1997-2000, 2004.

Mehta S., Grabowski T.J., Trivedi Y., Damasio H. Evaluation of voxel-based morphometry for focal lesion detection in individuals. *Neuroimage*, **20**: 1438-1454, 2003.

Nachev P., Coulthard E., Jager H.R., Kennard C., Husain M. Enantiomorphic normalization of focally lesioned brains. *Neuroimage*, **39**: 1215-1226, 2008.

Nagai M. and Kario K. Blood pressure, aging, vascular disease, and their effects on brain volume. *Am. J. Hypertens.*, **22**: 1135, 2009.

Oldfield R.C. The assessment and analysis of handedness: the Edinburgh Inventory. *Neuropsychologia*, **9**: 97-113, 1971.

Paus T., Tomaiuolo F., Otaky N., MacDonald D., Petrides M., Atlas J., Morris R., Evans A.C. Human cingulate and paracingulate sulci: pattern, variability, asymmetry, and probabilistic map. *Cereb. Cortex*, **6**: 207-214, 1996.

Pruessner J.C., Kohler S., Crane J., Pruessner M., Lord C., Byrne A., Kabani N., Collins D.L., Evans A.C. Volumetry of temporopolar, perirhinal, entorhinal and parahippocampal cortex from high-resolution MR images: considering the variability of the collateral sulcus. *Cereb. Cortex*, **12**: 1342-1353, 2002.

Rademacher J., Caviness V.S. Jr., Steinmetz H., Galaburda A.M. Topographical variation of the human primary cortices: implications for neuroimaging, brain mapping, and neurobiology. *Cereb. Cortex*, **3**: 313-329, 1993.

Raichle M.E. Behind the scenes of functional brain imaging: a historical and physiological perspective. *Proc. Natl. Acad. Sci. U.S.A.*, **95**: 765-772, 1998.

Ramon y Cajal S. *Textura del sistema nervioso del hombre y de los vertebrados*. 2 volumes. Madrid, Imprenta N Moya, 1899-1904.

Reggia J.A., Goodall S.M., Shkuro Y., Glezer M. The callosal dilemma: explaining diaschisis in the context of hemispheric rivalry via a neural network model. *Neurol. Res.*, **23**: 465-471, 2001.

Roland P.E. and Zilles K. Brain atlases--a new research tool. *Trends Neurosci.*, **17**: 458-467, 1994.

Rubens A.B., Mahowald M.W., Hutton J.T. Asymmetry of the lateral (sylvian) fissures in man. *Neurology*, **26**: 620-624, 1976.

Rudrauf D., Mehta S., Bruss J., Tranel D., Damasio H., Grabowski T.J. Thresholding lesion overlap difference maps: application to category-related naming and recognition deficits. *Neuroimage*, **41**: 970-984, 2008.

Schaechter J.D., Fricker Z.P., Perdue K.L., Helmer K.G., Vangel M.G., Greve D.N., Makris N. Microstructural status of ipsilesional and contralesional corticospinal tract correlates with motor skill in chronic stroke patients. *Hum. Brain Mapp.*, **30**: 3461-3474, 2009.

Schmitt O., Modersitzki J., Heldmann S., Wirtz S., Homke L., Heide W., Kompf D., Wree A. Three-dimensional cytoarchitectonic analysis of the posterior bank of the human precentral sulcus. *Anat. Embryol. (Berl).*, **210**: 387-400, 2005.

Shattuck D.W., Joshi A.A., Pantazis D., Kan E., Dutton R.A., Sowell E.R., Thompson P.M., Toga A.W., Leahy R.M. Semi-automated method for delineation of landmarks on models of the cerebral cortex. *J. Neurosci. Methods*, **178**: 385-392, 2009.

Slater R., Reivich M., Goldberg H., Banka R., Greenberg J. Diaschisis with cerebral infarction. *Stroke*, **8**: 684-690, 1977.

Small S.L. and Hoffman G.E. Neuroanatomical lateralization of language: sexual dimorphism and the ethology of neural computation. *Brain Cogn.*, **26**: 300-311, 1994.

Sowell E.R., Thompson P.M., Rex D., Kornsand D., Tessner K.D., Jernigan T.L., Toga A.W. Mapping sulcal pattern asymmetry and local cortical surface gray matter distribution in vivo: maturation in perisylvian cortices. *Cereb. Cortex*, **12**: 17-26, 2002.

Sporns O., Tononi G., Kotter R. The human connectome: a structural description of the human brain. *PLoS Comput. Biol.*, **1**: e42, 2005.

Steinmetz H., Furst G., Freund H.J. Variation of perisylvian and calcarine anatomic landmarks within stereotaxic proportional coordinates. *AJNR. Am. J. Neuroradiol.*, **11**: 1123-1130, 1990.

Steinmetz H. Structure, functional and cerebral asymmetry: in vivo morphometry of the planum temporale. *Neurosci. Biobehav. Rev.*, **20**: 587-591, 1996.

Swisher J.D., Halko M.A., Merabet L.B., McMains S.A., Somers D.C. Visual topography of human intraparietal sulcus. *J. Neurosci.*, **27**: 5326-5337, 2007.

Talairach J. and Tournoux P. *Co-planar stereotaxic atlas of the human brain. 3D proportional system: an approach to cerebral imaging*. New York, Georg Thieme Verlag, 1988.

Thompson P.M., Schwartz C., Lin R.T., Khan A.A., Toga A.W. Three-dimensional statistical analysis of sulcal variability in the human brain. *J. Neurosci.*, **16**: 4261-4274, 1996.

Toga A.W., Thompson P.M., Mega M.S., Narr K.L., Blanton R.E. Probabilistic approaches for atlasing normal and disease-specific brain variability. *Anat. Embryol. (Berl)*, **204**: 267-282, 2001.

Toga A.W., Thompson P.M., Mori S., Amunts K., Zilles K. Towards multimodal atlases of the human brain. *Nat. Rev. Neurosci.*, **7**: 952-966, 2006.

Toga A.W. and Thompson P.M. What is where and why it is important. *Neuroimage*, **37**: 1045-1049; discussion 1066-1048, 2007.

Tovino S.A. Imaging body structure and mapping brain function: a historical approach. *Am. J. Law Med.*, **33**: 193-228, 2007.

Van Essen D.C. and Dierker D.L. Surface-based and probabilistic atlases of primate cerebral cortex. *Neuron*, **56**: 209-225, 2007.

Van Hoesen G.W., Solodkin A., Hyman B.T. Neuroanatomy of Alzheimer's disease: Hierarchical vulnerability and neural system compromise. *Neurobiol. Aging*, **16**: 278-280, 1995.

Warabi T., Inoue K., Noda H., Murakami S. Recovery of voluntary movement in hemiplegic patients. Correlation with degenerative shrinkage of the cerebral peduncles in CT images. *Brain*, **113** (Pt 1): 177-189, 1990.

Watkins K.E., Paus T., Lerch J.P., Zijdenbos A., Collins D.L., Neelin P., Taylor J., Worsley K.J., Evans A.C. Structural asymmetries in the human brain: a voxel-based statistical analysis of 142 MRI scans. *Cereb. Cortex*, **11**: 868-877, 2001.

Weiller C., Isensee C., Rijntjes M., Huber W., Muller S., Bier D., Dutschka K., Woods R.P., Noth J., Diener H.C. Recovery from Wernicke's aphasia: a positron emission tomographic study. *Ann. Neurol.*, **37**: 723-732, 1995.

White L.E., Andrews T.J., Hulette C., Richards A., Groelle M., Paydarfar J., Purves D. Structure of the human sensorimotor system. I: Morphology and cytoarchitecture of the central sulcus. *Cereb. Cortex*, **7**: 18-30, 1997a.

White L.E., Andrews T.J., Hulette C., Richards A., Groelle M., Paydarfar J., Purves D. Structure of the human sensorimotor system. II: Lateral symmetry. *Cereb. Cortex*, **7**: 31-47, 1997b.

Wier H.Y., U. H., J.I. S., A. R., Small S.L. *Virtual Brain Transplantation: an approach for accurate registration and parcellation of brain-injured*

patients [Abstract]. In: Twelfth Annual Meeting of the Organization for Human Brain Mapping, Florence, Italy, 2006.

Yesilyurt B., Whittingstall K., Ugurbil K., Logothetis N.K., Uludag K. Relationship of the BOLD signal with VEP for ultrashort duration visual stimuli (0.1 to 5 ms) in humans. *J. Cereb. Blood Flow Metab.*, **30**: 449-458, 2010.

Zilles K., Schleicher A., Langemann C., Amunts K., Morosan P., Palomero-Gallagher N., Schormann T., Mohlberg H., Burgel U., Steinmetz H., Schlaug G., Roland P.E. Quantitative analysis of sulci in the human cerebral cortex: development, regional heterogeneity, gender difference, asymmetry, intersubject variability and cortical architecture. *Hum. Brain Mapp.*, **5**: 218-221, 1997.